



The DSCOVR-EPIC (Earth Polychromatic Imaging Camera) is a refurbished version of an instrument developed for the original suspended Triana 2001 mission instrument. The key changes made to EPIC were improved field group optics and anti-reflection coatings to reduce stray light and new filters with anti-reflection coatings. The logo above shows EPIC deployed atop the DSCOVR spacecraft with the telescope cover door open to permit a view of the earth while the solar side instruments monitor solar activity. Also shown is the adjacent NISTAR cavity radiometer that will be discussed in a separate document.

A schematic diagram of the DSCOVR spacecraft's view of the Earth from the orbit around the Earth-Sun Lagrange-1 point, 1.5 million kilometers from the Earth. The orbit is a non-repeating Lissajous figure tilted with respect to the Earth's ecliptic plane. It takes 6 months for one circuit during which the apparent size of the earth varies about the nominal size of 0.5 degrees (Epic has a field of view of 0.62 degrees). While the mission is planned for 2 years, during the extended life of the mission the orbital shape will change from an approximate ellipse to an approximate circle and then back to an ellipse in approximately 5 years. The orbit at L-1 is quasi-stable, and requires periodic corrections from onboard rocket (hydrazine) motors. This would be the case even without the strong perturbations from the Earth's moon. More information on the orbit will be given in a separate document.

The following figures present an overview summary of DSCOVR-EPIC.

Contact	Adam Szabo (Project Scientist)	Adam.Szabo-1@nasa.gov
Contact	Alexander Marshak (Associate Project Scientist)	Alexander.Marshak@nasa.gov
Contact	Jay Herman (EPIC Instrument Scientist)	Jay.R.Herman@nasa.gov

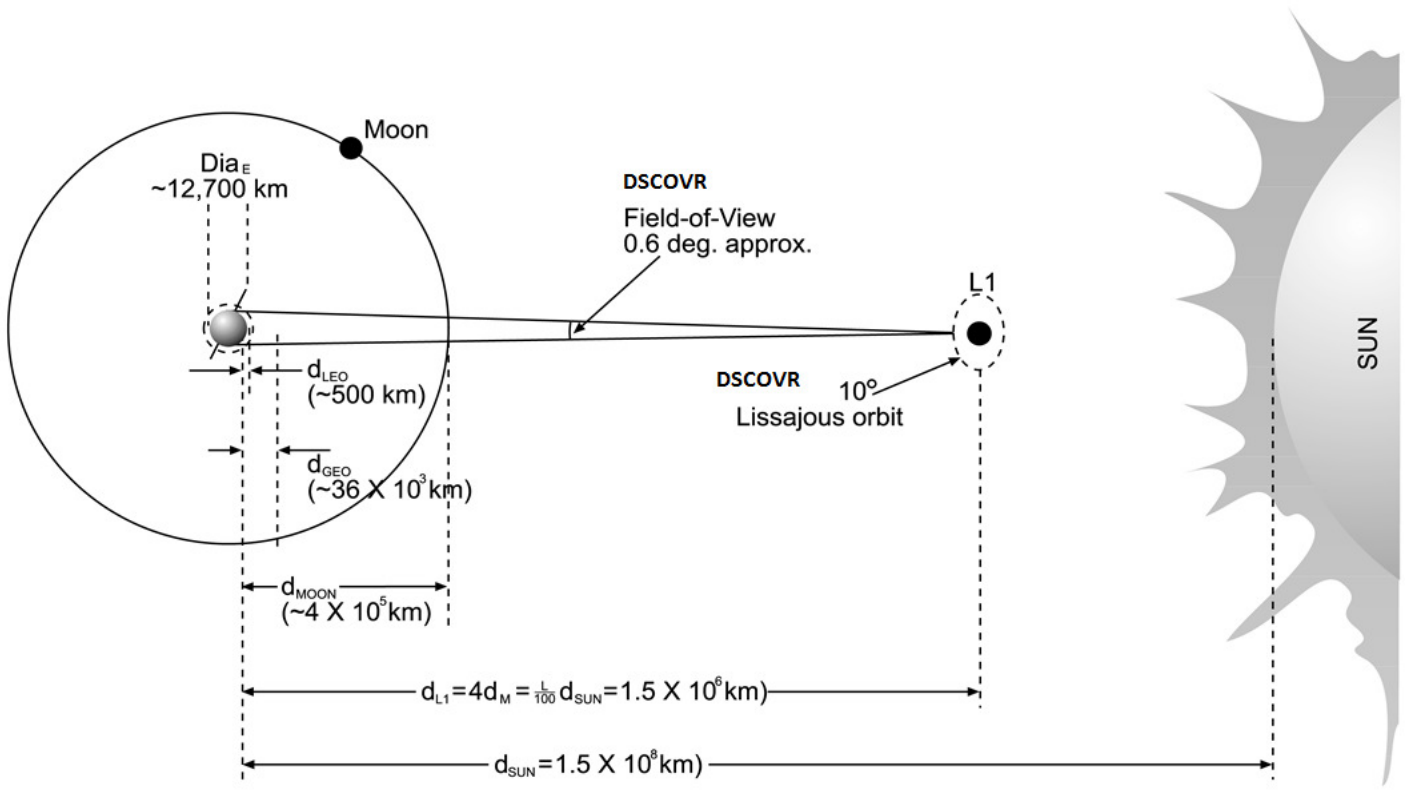


Figure 1 Schematic of DSCOVR orbit at Lagrange-1 showing the basic Earth-viewing geometry.

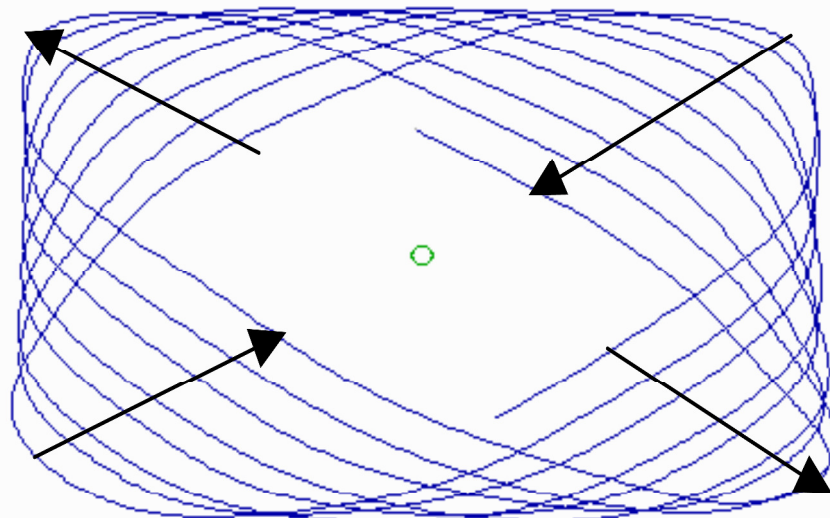


Figure Idealized non-repeating Lissajous orbit about the Earth-Sun line. Each approximate circuit takes 6 months. The actual orbit irregular because of perturbations from the Moon and from periodic orbit maintenance adjustments.

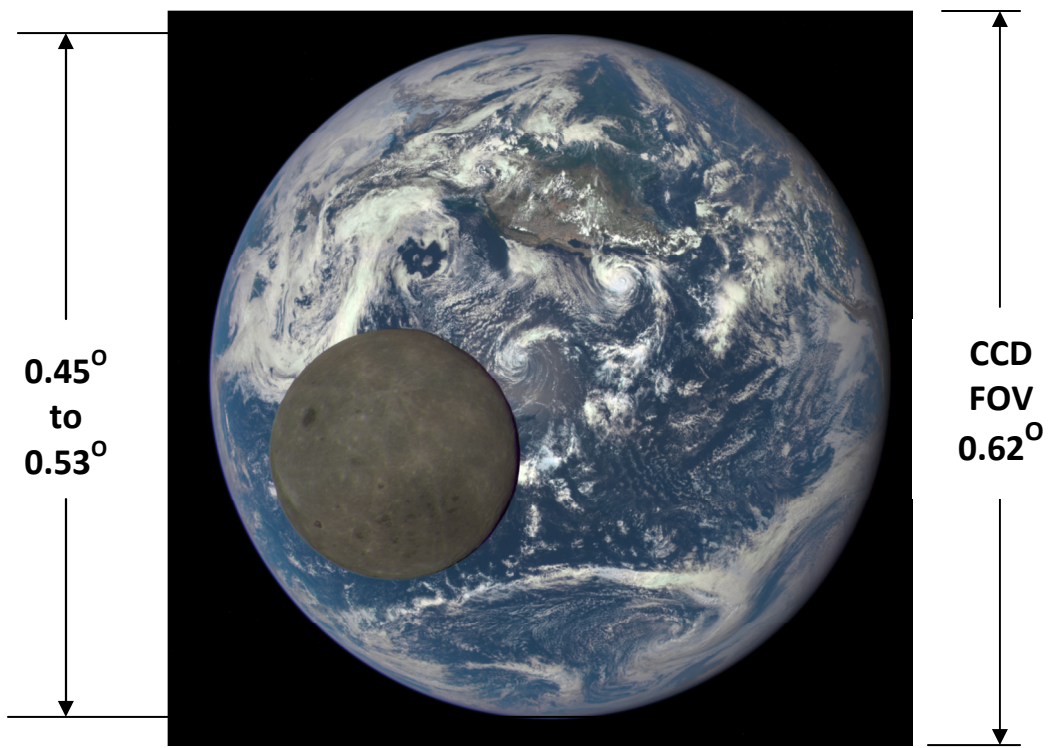
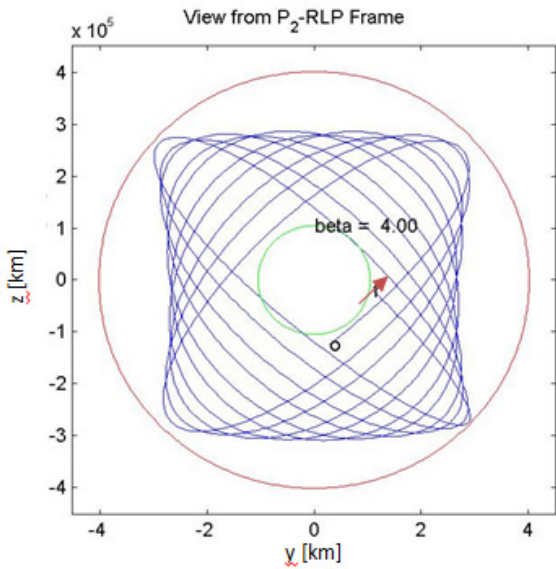


Figure 2 EPIC view of the Earth and Moon from L1 on July 16, 2015

Lissajous Orbit Viewed from Earth

($15^\circ, 15^\circ, 4^\circ$) Class 2/CCW, 5 years
6 month period for a single loop



Size and angles of the Lissajous orbit at L1

Angle between Sun-Earth line & position vector from Earth to Vehicle (SEV Angle)

or

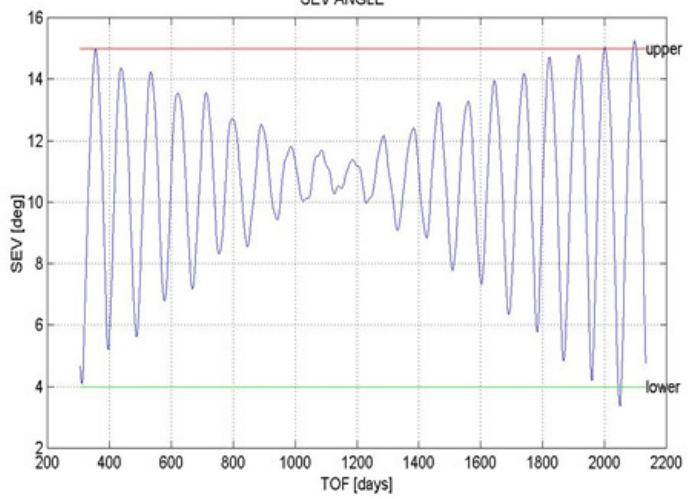
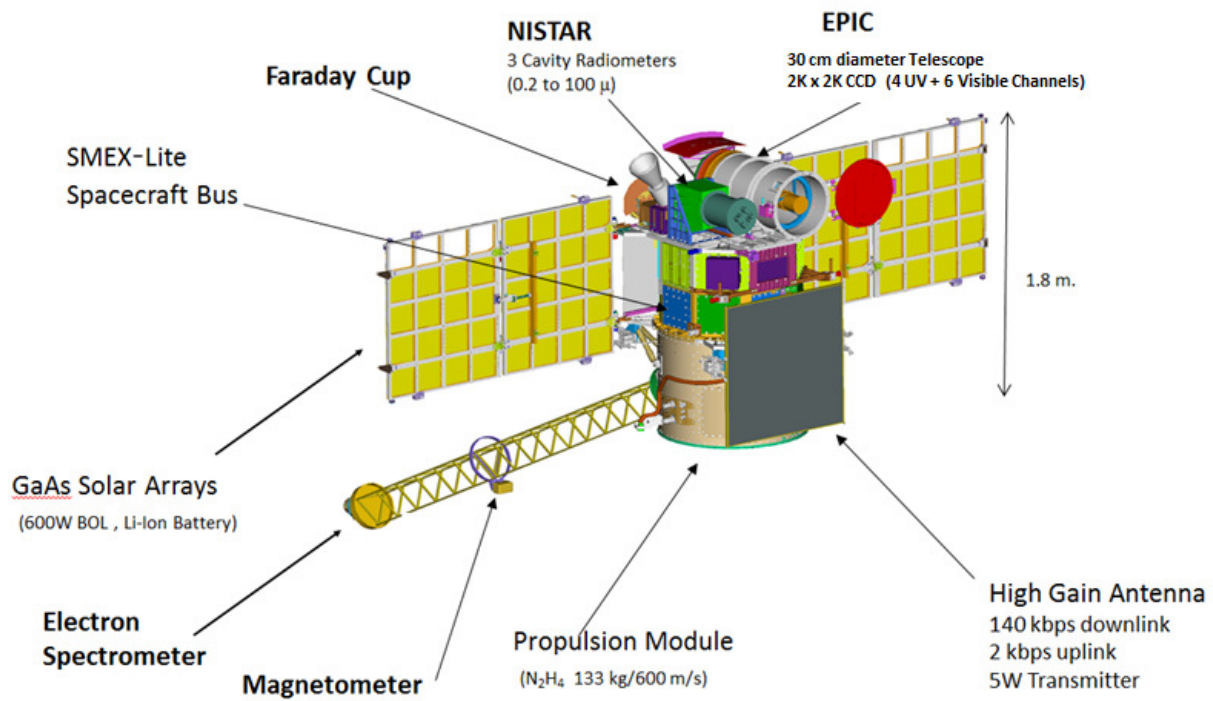




Figure 3 A simulated view of the Moon when it may be used for EPIC stability analysis. During in-flight calibration, the Moon will be located between 2 to 8 Earth diameters from the limb of the Earth. EPIC stability will be estimated using the reflectivity of the lunar surface as a function of wavelength at the appropriate solar zenith angles. The reflectivity will be obtained from the Lunar Reconnaissance Orbiter (LRO) and from USGS ROLO data.



Schematic view of the DSCOVR observatory showing the relative positions of EPIC, NISTAR, the solar electrons spectrometer, faraday cup, and magnetometer, solar arrays, and flat panel antenna.

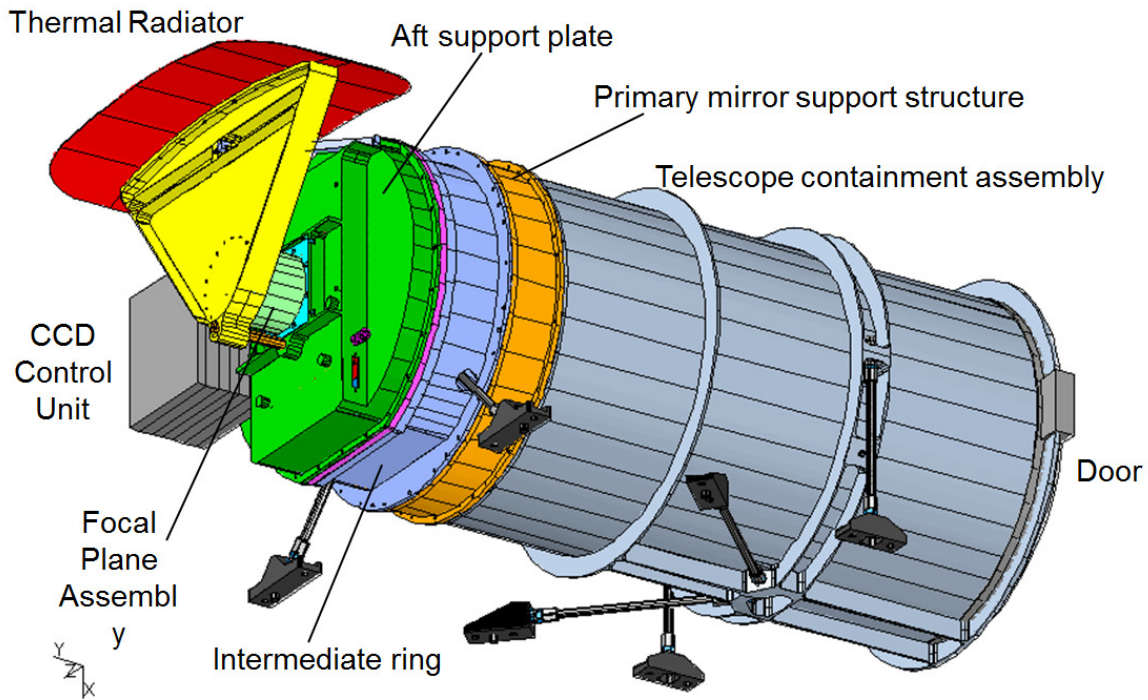
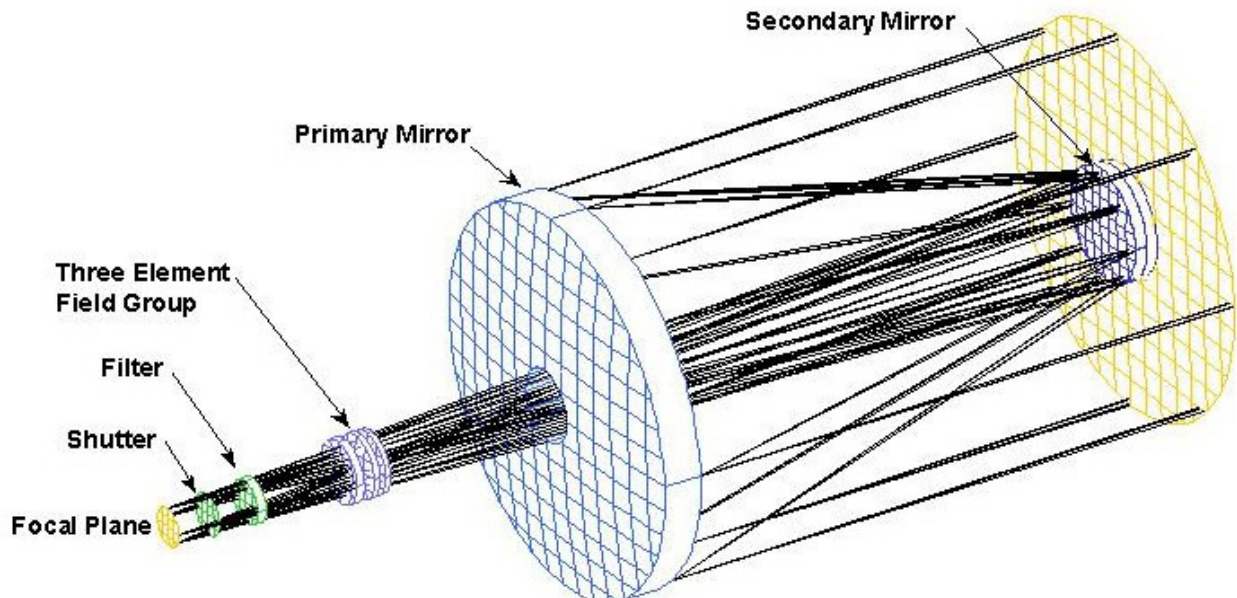
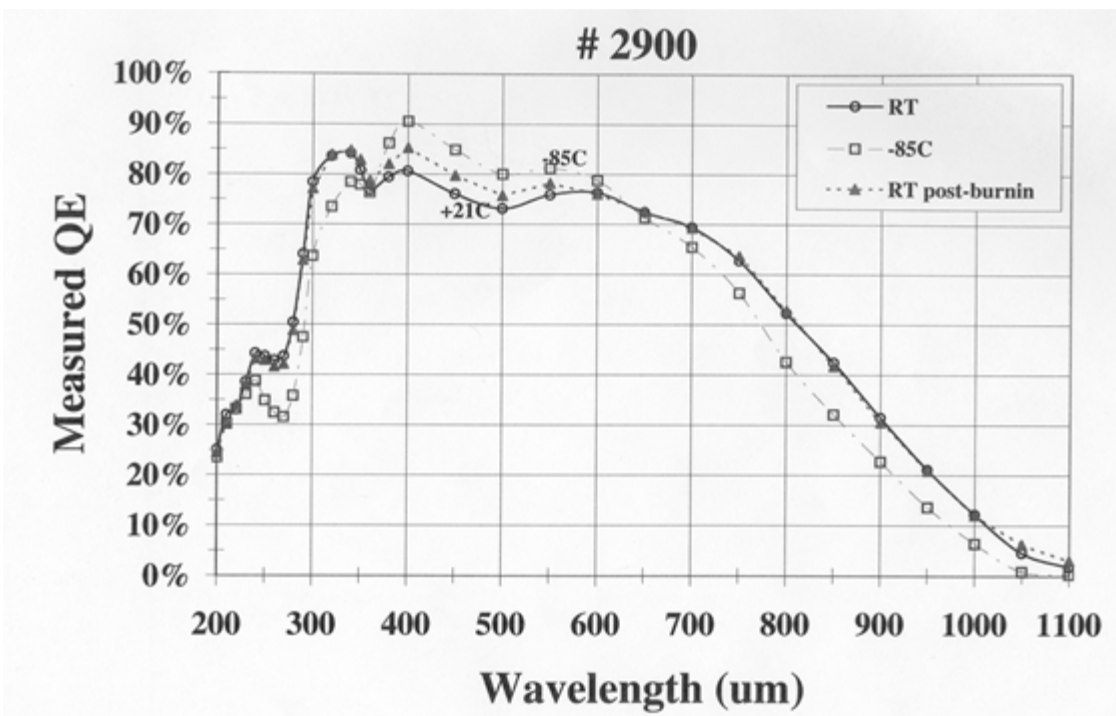


Figure xx View of the EPIC spectroradiometer showing the external housing for the 30 cm telescope and the thermal radiator attached to the charge coupled device (CCD) housing to keep the CCD at about -40°C . The six struts are for attachment to the spacecraft.

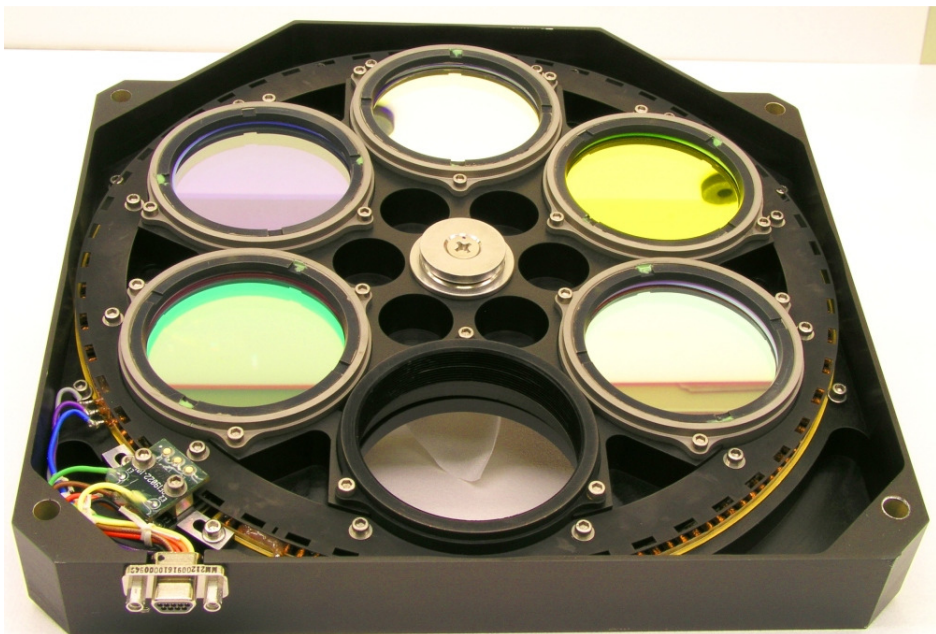


Schematic of EPIC telescope design showing the relative positions of the primary and secondary mirrors, the focusing 3-element field lens group, the 12 position dual filter wheels, the rotating shutter, and the CCD focal plane

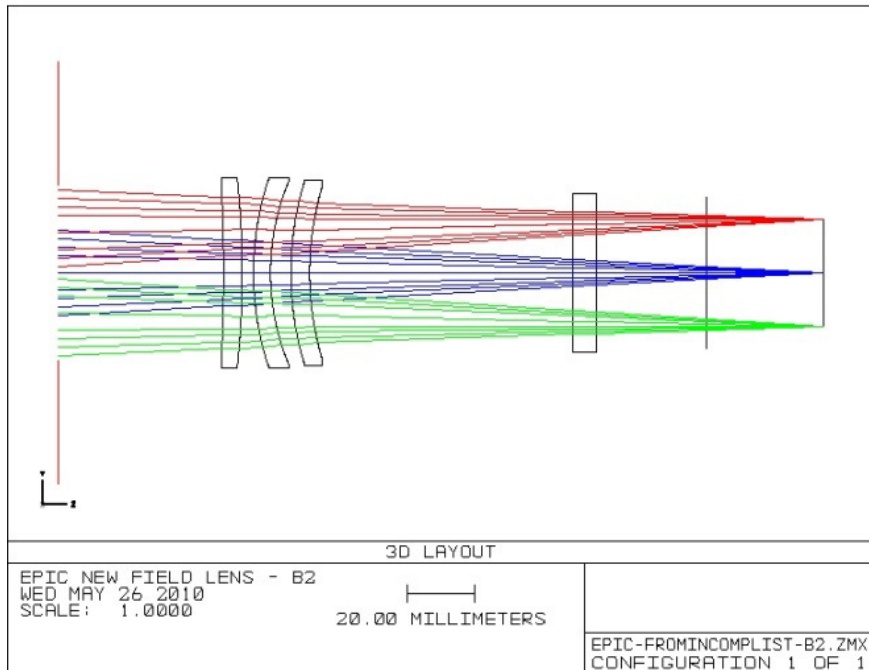


Michael Lesser
University of Arizona

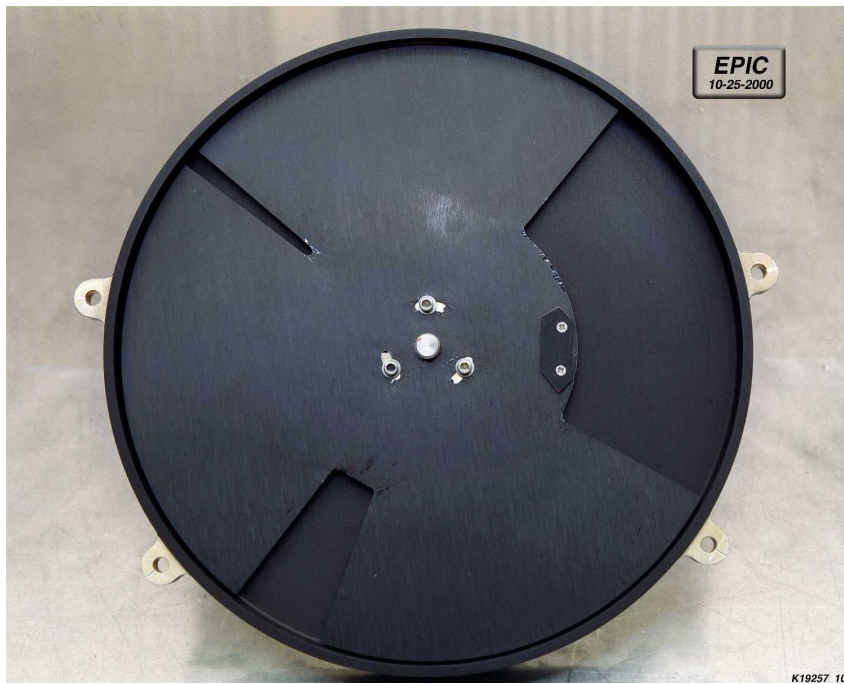
Quantum Efficiency of CCD detector at -85C and + 21C. Nominal operating temperature -40C.



Filter Wheels showing 5 filters per wheel plus 1 open hole position per wheel.



Schematic of EPIC field lens group optimized to minimize ghosting



Rotating shutter assembly showing the 3 slits possible for selecting different exposure times. In practice, only the two larger slits will be used because of exposure non-uniformity across the CCD when using the smallest slit. Final exposure times will be determined on orbit so that the CCD wells are filled to about 80% for each wavelength channel to provide maximize signal to noise and prevent blooming from overfilling the wells.

Table EPIC center wavelengths for the 10 filters

λ (nm)	FWHM (nm)	Nominal Product
317.5 ± 0.1	1 ± 0.2	<i>Ozone</i>
325 ± 0.1	2 ± 0.2	<i>Ozone</i>
340 ± 0.3	3 ± 0.6	<i>Ozone, Aerosols, Clouds</i>
388 ± 0.3	3 ± 0.6	<i>Aerosols, Clouds</i>
443 ± 1	3 ± 0.6	<i>Aerosols</i>
551 ± 1	3 ± 0.6	<i>Aerosols, Vegetation</i>
680 ± 0.2	2 ± 0.4	<i>Aerosol, Vegetation, Clouds, O_2 B-Band Reference</i>
687.75 ± 0.2	0.8 ± 0.2	<i>O_2 B-Band Cloud Height</i>
764.0 ± 0.2	1 ± 0.2	<i>O_2 A-Band Cloud Height, Aerosol Height</i>
779.5 ± 0.3	2 ± 0.4	<i>O_2 A-Band Reference, Vegetation</i>

Calibration and Stray Light

DSCOVR EPIC has no capability for onboard calibration.

There are 4 basic issues to consider.

- 1) CCD flatfielding
- 2) Dark Current
- 3) Radiometric calibration of the various filter channels
- 4) Correction for stray light
- 5) Etalonning (interference effects within the CCD at wavelengths longer than 600 nm)

CCD Flatfielding

Measurements of CCD uniformity were performed while the instrument was being refurbished. A pixel by pixel map exists giving the relative sensitivity of one pixel relative to another for the entire 2048 x 2048 CCD. Originally, a check on flatfielding was going to be performed using a statistical method based on lunar observations. Given current telemetry restrictions, this method is not possible. Fortunately, experience with CCD detectors on OMI and NPP have shown that CCD flatfielding appears to be stable except for the development of hot pixels and dark pixels. Hot pixels will be detected during the periodic dark current measurement. Dark pixels are more of a problem, since there is no uniform onboard light source. Manual inspection of Earth images may be necessary

Dark Current

Once per month, measurements will be made with the shutter closed for periods equivalent to the normal exposure time when viewing the Earth or Moon. The exposure time will vary to match the exposure used for the various filters.

Radiometric calibration of the various filter channels

Radiometric calibration will be obtained from images of the Moon for each filter when the Moon is between 2 to 4 degrees away from the Earth's center (4 to 8 Earth diameters). Exposures will be adjusted for each filter channel so that the CCD well is filled to approximately 80% for best signal to noise readings. Lunar surface reflectivity will be determined from external data such as from the Lunar Reconnaissance Orbiter (LRO) and the USGS ROLLO project at the appropriate view angles (~170 degrees). The project will supply the initial lunar calibration obtained during the first month of operation at L1. Subsequent lunar calibration images will be used to check instrument radiometric stability.

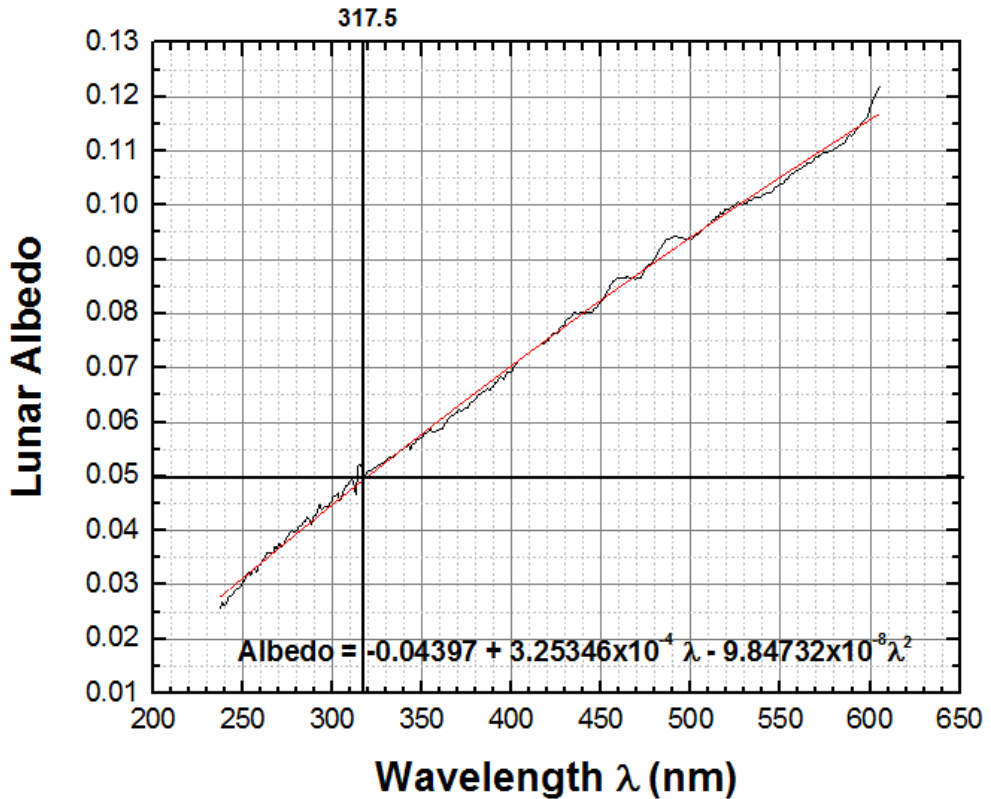


Figure A preliminary estimate of lunar albedo as a function of wavelength derived from GOME satellite measurements. These estimates will be supplemented with LRO and ROLLO data obtained at the appropriate view and solar zenith angles.

The lunar albedo data will be used to convert counts into radiances by using the known solar flux striking the moon, accounting for limb darkening, the overall efficiency of the EPIC system, correcting for geometrical effects related to the relative positions of the DSCOVR satellite and Moon, and the pixel to pixel differences in sensitivity (flat fielding).

Correction for Stray Light

Stray light affects every pixel on the detector to varying degrees in an amount that makes retrieval of some products (e.g., ozone) not useful without correction. The sources of stray light are primarily from reflections in the field lens group, reflections between the filter surfaces and the shiny CCD surface, and from some of the support structures within the telescope. During the refurbishment of EPIC extensive measurements were made of the stray light patterns that occurred for different sizes of light sources. The EPIC project has attempted to perform a detailed analysis of the stray light, the instrument point-spread function, and diffraction effects. The end result is an algorithm that should be able to correct the stray light sufficiently to make accurate retrievals of geophysical quantities feasible. The correction algorithms will run on the project's computers as part of the Level-1 processing to produce calibrated counts and radiances.

The problem is made worse by the varying amount of light that arises from the distribution of cloudy and clear scenes of very different brightness. A sample scene is shown below with errors in measured radiances of +/- 18% in the indicated small box.

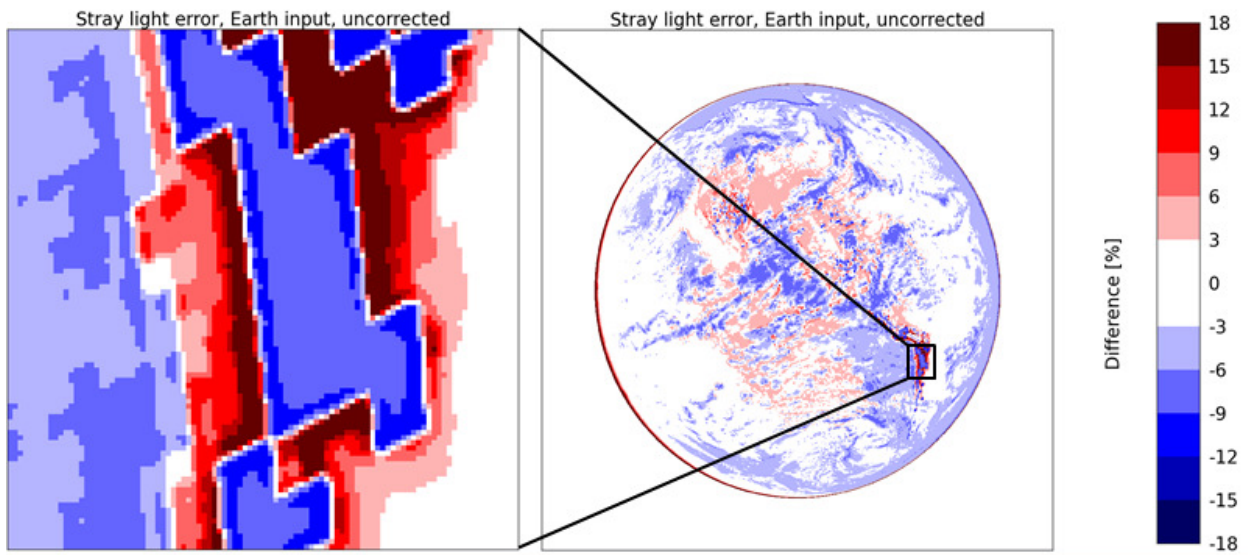


Figure The effect of stray light arising from cloudy scenes on a portion of the scene that is cloud free.

The problem is “solved” by determining the point-spread function in the laboratory using different size targets, determining the stray light effect associated with different size targets, and identifying as many of the sources of internal reflection as possible. An example of the point-spread function PSF is shown in the figure below.

In order to proceed with the stray light correction algorithm, a first guess estimation of the PSF for each filter and all pixels was made. All the PSFs are combined into a spread matrix. The inversion of the spread matrix is the stray light correction matrix C . C will be applied on the measured counts r to obtain the stray light corrected counts r_C . The problem is that there are 2048x2048 pixels leading to a matrix C that is huge (4161600×4161600), which necessitates special treatment and the use of a super computer

to perform the inversion. Fortunately C is diagonally dominant so that it can be represented by $I + D$, where I the unit matrix. The inversion can then be determined by $C = (I + D)^{-1} = I - D + D^2 - D^3 + D^4 \dots$. This still represents a very large problem, but one that only has to be solved once based on laboratory data, and then, perhaps, again if there is suitable data obtained while in orbit.

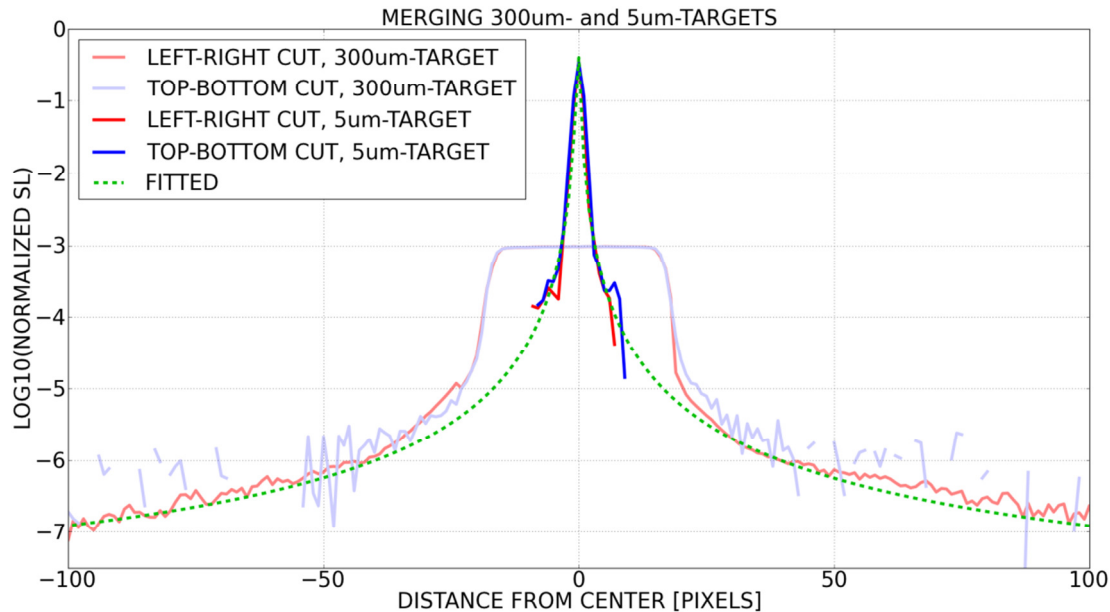


Figure The effective point spread function determined in the laboratory. Optical modeling was used to confirm the laboratory results.

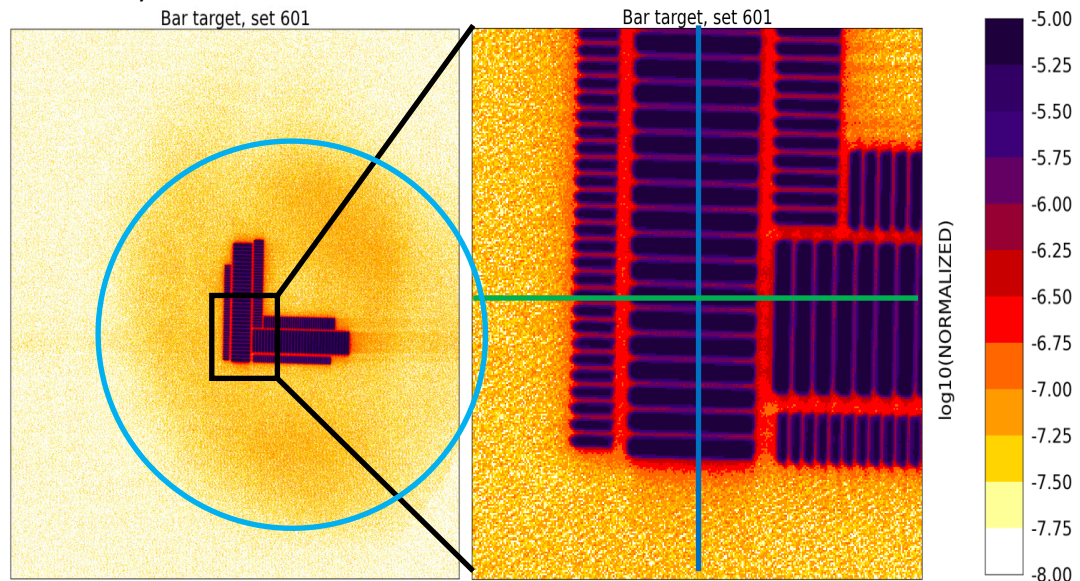


Figure An example of uncorrected data is shown in an image of a bar chart that is magnified in the right hand panel. The red areas are composed of stray light. When corrected, the red areas will be removed.

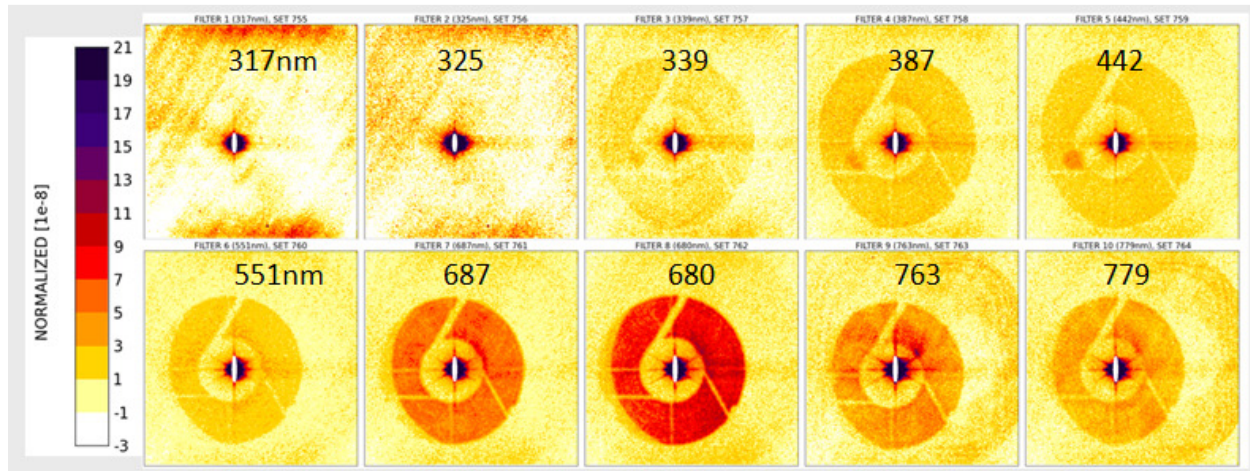


Figure Laboratory measured stray light for each of the 10 filter channels. Clearly shown are the secondary mirror support structure (spider), interference effects, and ghosting (reflections from various optical surfaces).

Using simulated data we have tested the stray light correction method. The correction reduces the stray light substantially (see right panel below) to a degree that is much better than will be achieved with in-orbit measured radiances. The method is expected to reduce measured stray light effects to less than 1%, which is sufficient for proposed science algorithms.

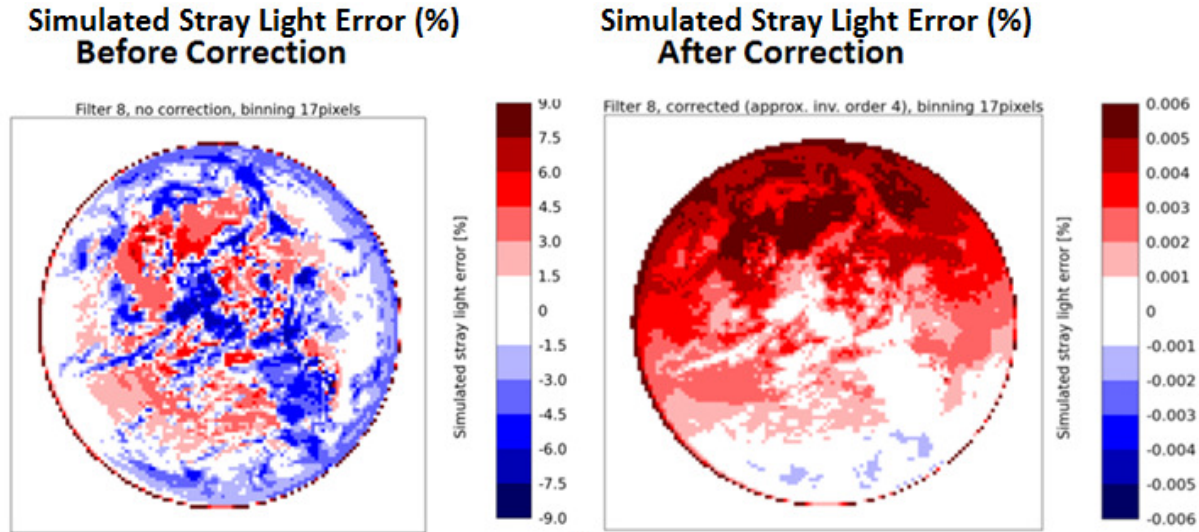


Figure A demonstration of the stray light correction algorithm applied to simulated data.

Etaloning

For longer wavelengths (> 600 nm) silicon becomes increasingly transparent. This permits interference effects between the front and back surface of the CCD. Since the interference patterns are expected to

be stable, they can also be corrected by an independent algorithm. An example is shown in the next figure, which compares the stray light seen with a 300 micron target for the 317 nm and 763 nm channels. There are two effects easily seen in this figure. First, are the interference fringes seen for 763 nm and second is the “shadow” effect that arises from the left to right readout method on the CCD. The stable “shadow effect is present in all channels, but most easily seen in 317 nm, and will also be corrected as part of the stray light correction.

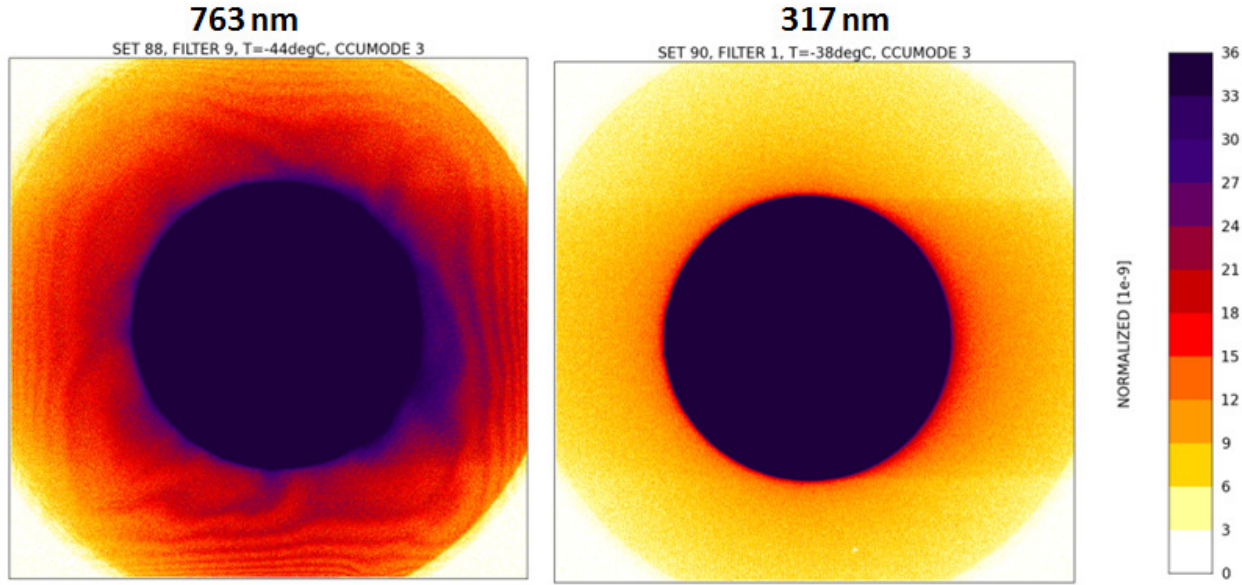


Figure An example of the etaloning effect for 763 nm and the readout “shadow” effect for 317 nm. The shadow effect is also seen for 763 nm.